Electronic supplementary information

A Simple Approach In Achieving A Metastable Metal Oxide Derived from Carbonized Metal-Organic Gels

Jing-Cheng Huang[a], Yung-Han Shih[a], Stephen Lirio[a], Shiuan-Yau Wu[a], Hsin-Tsung Chen[a], Wan-Ling Liu[a,b*], Chia-Her Lin[a,c*] and Hsi-Ya Huang[a,†]

[a] Department of Chemistry, Chung Yuan Christian University, 200 Chung Pei Rd., Chungli District, Taoyuan City, 320, Taiwan. E-mail: chiaher@cycu.edu.tw

[b] College of Science, Chung Yuan Christian University, 200 Chung Pei Road, Chung Li District, Taoyuan City, 320, Taiwan. E-mail: wendyliu@cycu.edu.tw

[c] R&D Center for Membrane Technology Chung Yuan Christian University, 200 Chung Pei Road, Chung-Li District, Taoyuan City, 320, Taiwan

[†] Deceased August 22, 2017

Experimental Section

Materials

The dopamine hydrochloride (Da), D/L-norepinephrine hydrochloride (Ne), (-)- epinephrine (E), palmitate acid, methyl linoleate (internal standard), methyl palmitate and amino acids (arginine (Arg), histidine (His), lysine (Lys), aspartate (Asp), glutamate (Glu)) were purchased from Sigma-Aldrich. Zirconium tetrachloride nonhydrate ($ZrCl_4$) was purchased from Alfa Aesar. The 1,4-benzenedicarboxylic acid (H_2BDC) was purchased from Showa Chemical Co., Ltd while N,N-Dimethylformamide (DMF, >99%) was purchased from Honeywell Research Chemicals. The ethanol (EtOH, 95 %) was purchased from ECHO chemicals.

Apparatus

The MOG synthesis was carried out in a reaction using Circulator Oven (DK-30NP2, YOTEC) and calcined in tubular furnaces (OT-T060, Olink). X-ray diffractometer (Bruker D8 Advance ECO, Bruker Daltonics) was used for characterizing the materials. A scanning electron microscope (JSM-7600F, JEOL) was used to verify the morphology of the synthesized MOGs. Raman spectrometer (Triax 320, Jobin Yvon) was used to evaluate the degree of graphitization of nanoporous carbon materials (NPCs). X-ray photoelectron spectroscopy (XPS, VG Scientific ESCALAB 250, UK) from National Taiwan University was utilized for surface determination of NPCs. An autoflex Speed MALDI-TOF mass spectrometer (Bruker Daltonics, Germany) was used for the determination of analytes using 355 nm Nd:YAG-laser at 100 Hz. The biodiesel product was determined by GC-FID (GC-7890, Agilent).

Preparation of Zr-MOG

The zirconium MOG was synthesized according to the previous literature.[S1] Typically, a mixture of zirconium tetrachloride nonahydrate ($ZrCl_4$, 0.0466 g, 0.2 mmol), 1,4-benzenedicarboxylic acid (C_6H_4-1,4-$(CO_2H)_2$, H_2BDC, 0.0332 g, 0.2 mmol), dimethylformamide (DMF, 0.5 mL) and ethanol (EtOH, 0.5 mL) in a 23 mL Teflon autoclave. The mixture was heated at 80 ºC then kept for 4.5 h. After cooling to room temperature, the white gel were obtained and activated in ethanol then dried overnight at 80 ºC.

Preparation of carbonized MOGs

The MOG powders (0.2 g) were placed in a ceramic boat then transferred in the tube furnace. The furnace was heated from room temperature to 600, 700, 800 and 900 ºC (hereafter denoted as ZrO_2-NPC-X in which X = temperature) at heating rate of 5 ºC min^{-1} under $N_{2(g)}$ condition. After reaching the specified temperature, it was kept for 5 h and then cool down to room temperature at rate of 1 ºC min^{-1}.

Sample preparation for LDI process

A 100 mg L^{-1} stock solution containing Da, E and Ne were dissolved in deionized water (D.I. water) followed by ultrasonication in ice bath for 10 mins and stored at 4 ºC prior to use. In a separate container, a 2000 mg L^{-1} matrix solution containing Zr-MOGs or ZrO_2-NPC was suspended in 100 µL EtOH/H_2O (v/v, 1:1). For LDI assay, 1 µL matrix solution was placed onto the target plate and allowed to dry at room temperature. Thereafter, 1 µL sample solution was deposited onto the matrix surface and dried at room temperature.

Esterification reaction of free fatty acid (FFA)

A 0.22 mmol (56 mg) of palmitate was dissolved in 0.8 mL methanol (molar ratio is 1 : 90), and added with 18 wt% (10 mg) ZrO_2-NPC-800, as catalyst, in a batch reactor. The reaction temperature was set at 68 ℃ for 24h. After reaction, the mixture was centrifuged and collected biodiesel products (*i.e.*, supernatant). The products were diluted to 100 mg L^{-1} and analyzed by GC-FID. The recyclability of the catalyst was carried out by washing it with methanol and dried for next catalytic cycle.

Computational Methods

All structure optimizations have been carried out with DFT plane-wave calculations as implemented in the Vienna Ab initio Simulation Program (VASP). A cutoff energy of 450 eV was set for a plane-wave basis. The Brillouin zone was sampled with (3 × 3 × 1) k-point mesh for surface calculations. The (-111) and (101) surfaces with a vacuum space of 15 Å were modeled for monoclinic ZrO_2 and tetragonal ZrO_2, respectively.

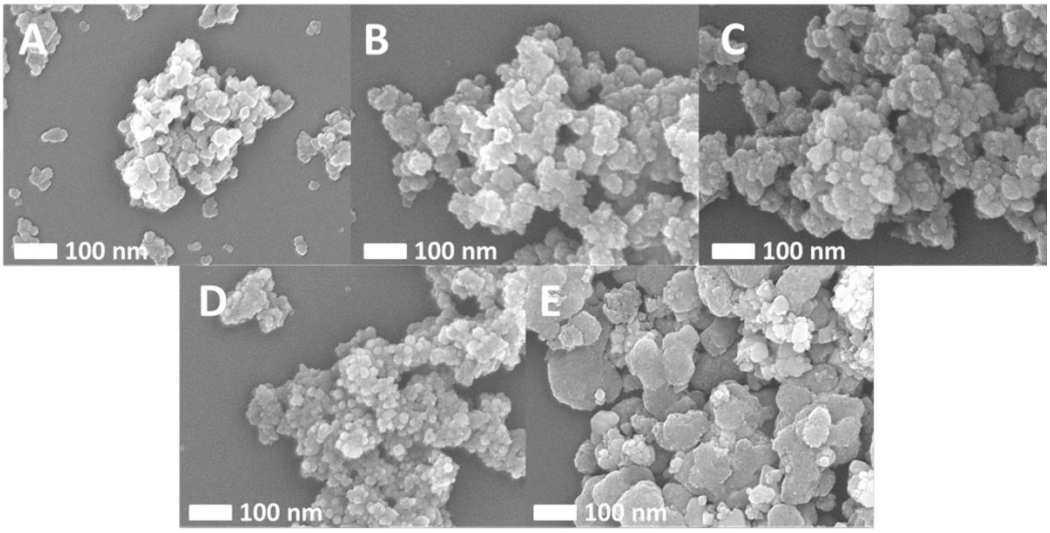

Fig S1. SEM images A) Zr-MOG, B) ZrO_2-NPC-600, C) ZrO_2-NPC-700, D) ZrO_2-NPC-800, and E) ZrO_2-NPC-900.

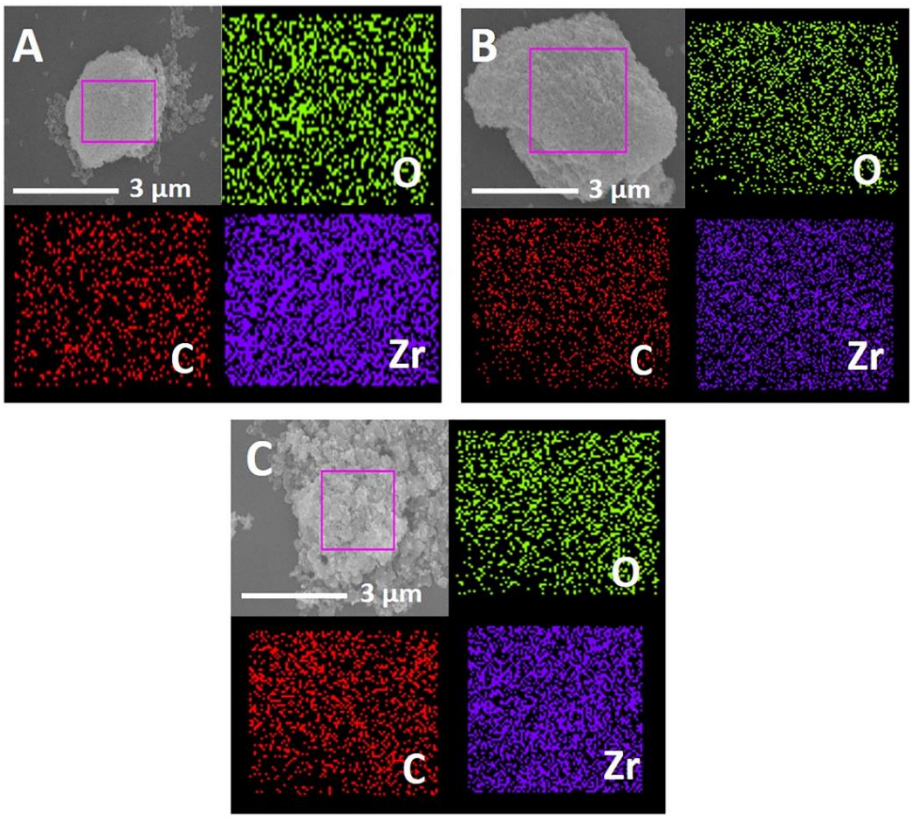

Fig S2. SEM-EDS micrographs of A) ZrO_2-NPC-600, B) ZrO_2-NPC-700 and C) ZrO_2-NPC-900.

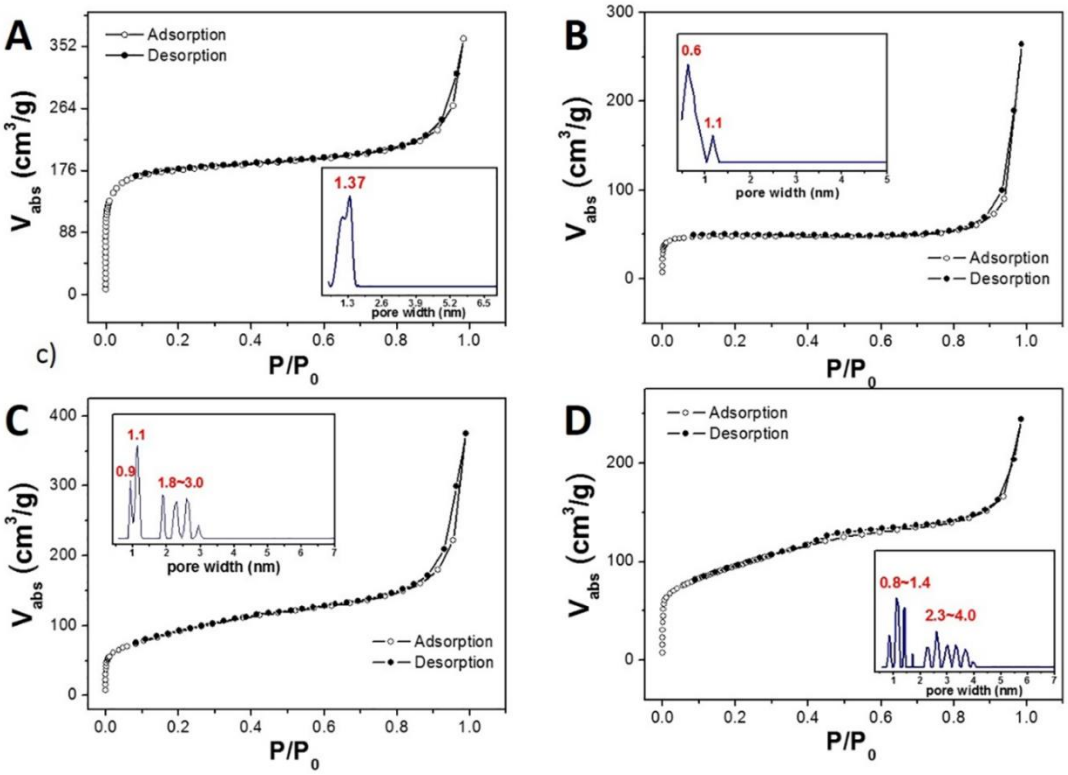

Fig S3. N_2 sorption isotherms and pore size distribution of A) Zr-MOG, B) ZrO_2-NPC-600, C) ZrO_2-NPC-700 and D) ZrO_2-NPC-900.

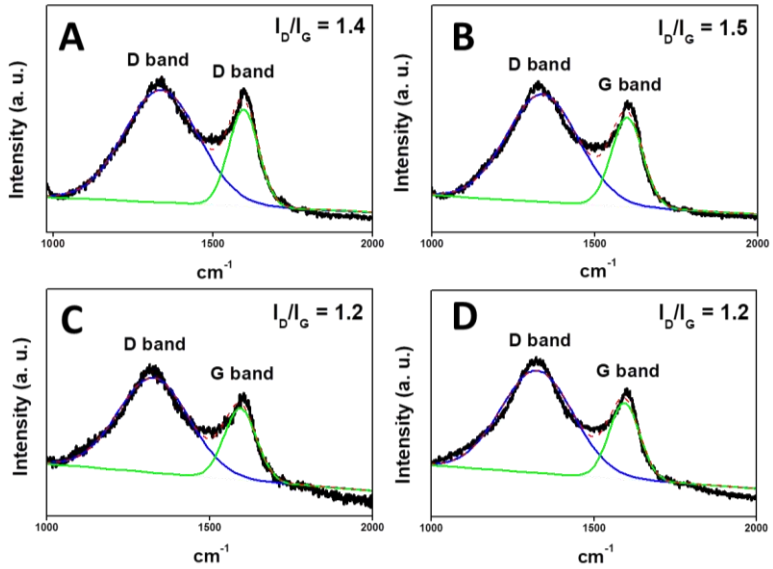

Fig S4. Curve fitting of Raman spectrums for ZrO_2-NPC carbonized at A) 600 ºC, B) 700 ºC, C) 800 ºC and D) 900 ºC. The I_D/I_G ratio are calculated via peak intensity after curve fitting.

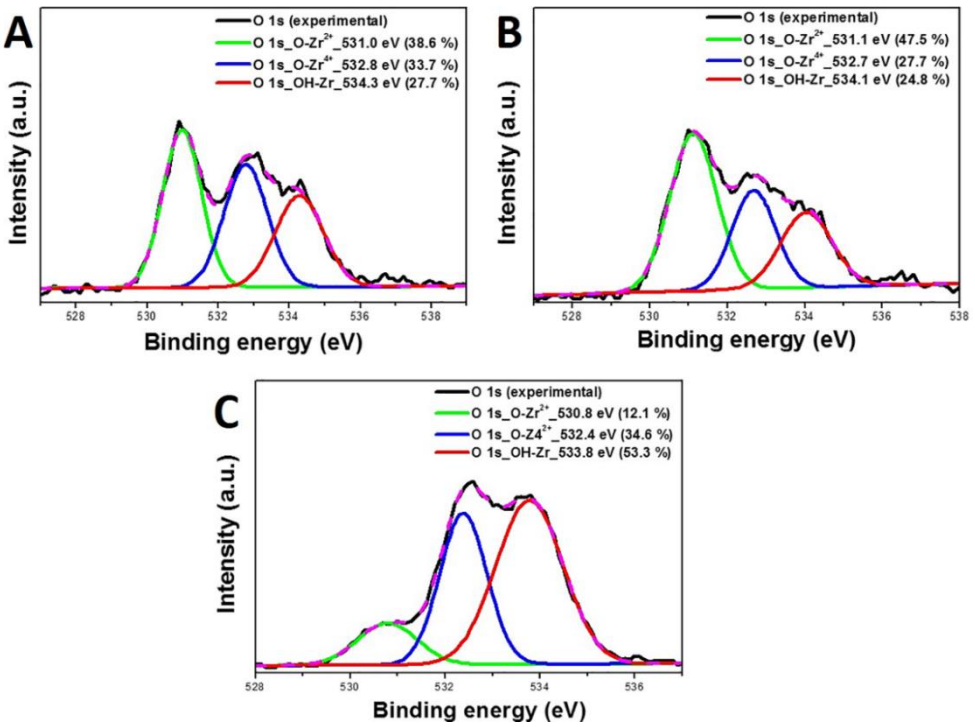

Fig S5. XPS spectras were obtained from curved fitting of O 1s A) ZrO_2-NPC-600, B) ZrO_2-NPC-700, and C) ZrO_2-NPC-900.

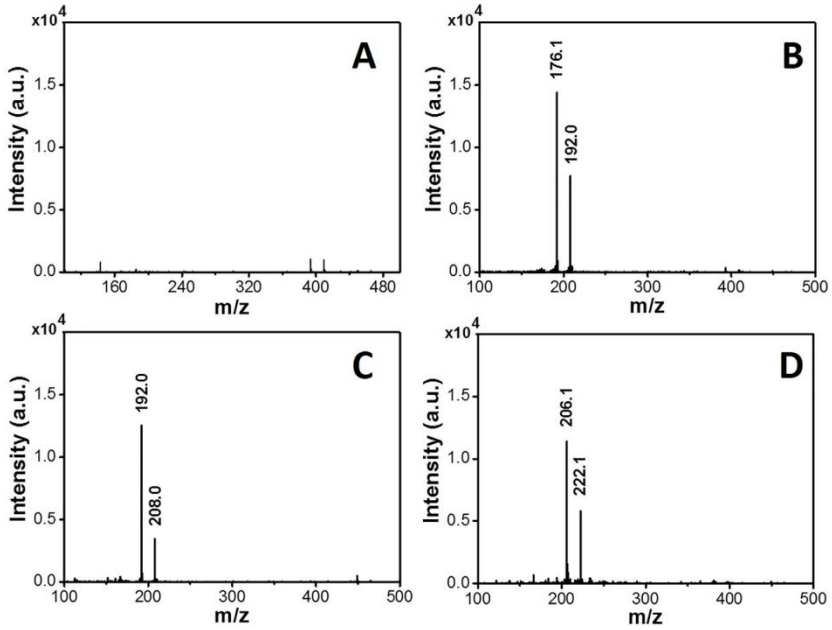

Fig S6. SALDI-MS spectras of A) blank, B) Da ($[M+Na]^+$, m/z 176.1; $[M+K]^+$, m/z 192.0), C) Ne ($[M+Na]^+$, m/z 192.0; $[M+K]^+$, m/z 208.0), D) E ($[M+Na]^+$, m/z 206.1; $[M+K]^+$, m/z 222.1). Matrix: ZrO_2-NPC-600. Detection: *Positive ion mode*. Laser conditions: 30 %, 500 shots. N=10

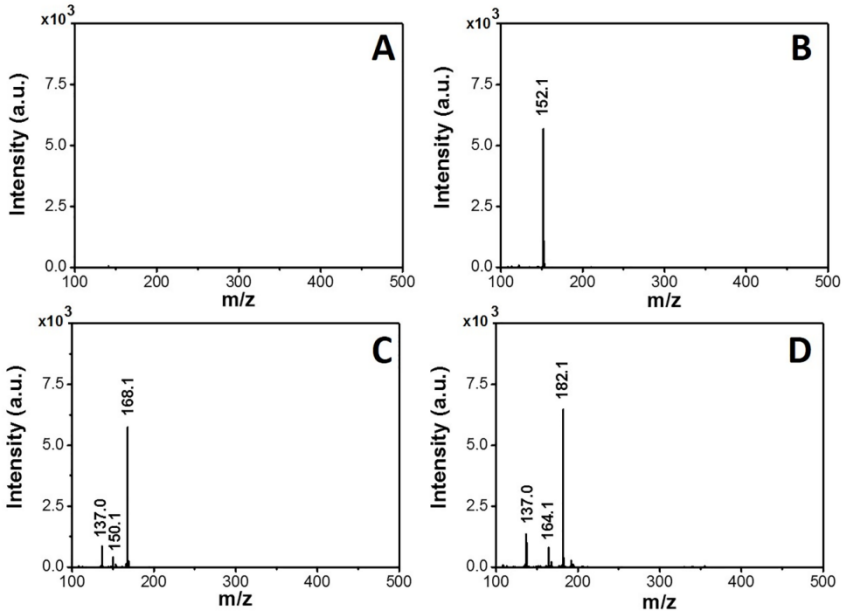

Fig S7. SALDI-MS spectras of A) blank, B) Da ([M-H]$^-$, m/z 152.1),C) Ne ([M-H]$^-$, m/z 168.1; [M-H_2O-H]$^-$, m/z 150.1; [M-CH_2NH_2-H]$^-$, m/z 137.0),D) E ([M-H]$^-$, m/z 182.1; [M-$CH_3CH_2NH_2$-H]$^-$, m/z 137.0). Matrix: ZrO_2-NPC-600. Detection: *Negative ion mode*. Laser conditions: 30 %, 500 shots. N=10

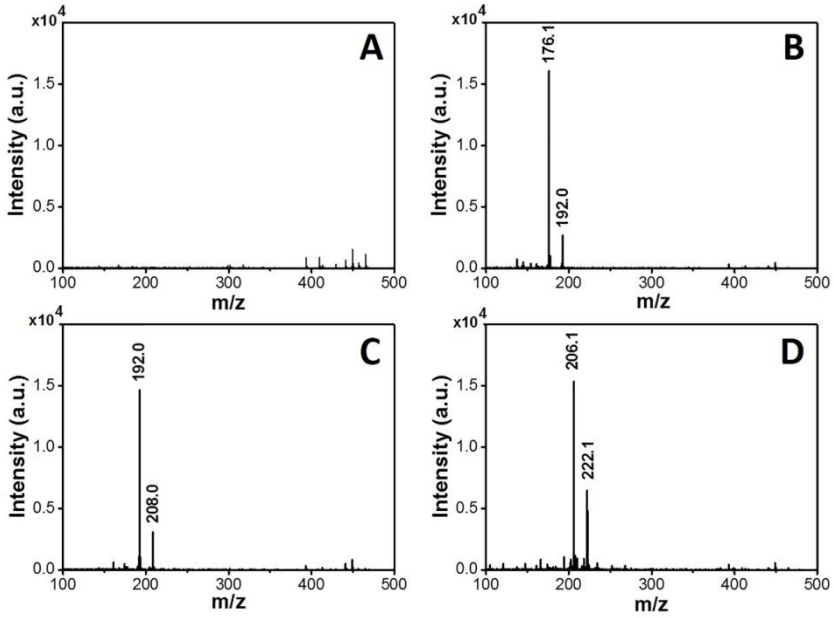

Fig S8. SALDI-MS spectras of A) blank, B) Da ([M+Na]$^+$, m/z 176.1; [M+K]$^+$, m/z 192.0), C) Ne ([M+Na]$^+$, m/z 192.0; [M+K]$^+$, m/z 208.0), D) E ([M+Na]$^+$, m/z 206.1; [M+K]$^+$, m/z 222.1). Matrix: ZrO_2-NPC-700. Detection: *Positive ion mode*. Laser conditions: 30 %, 500 shots. N=10

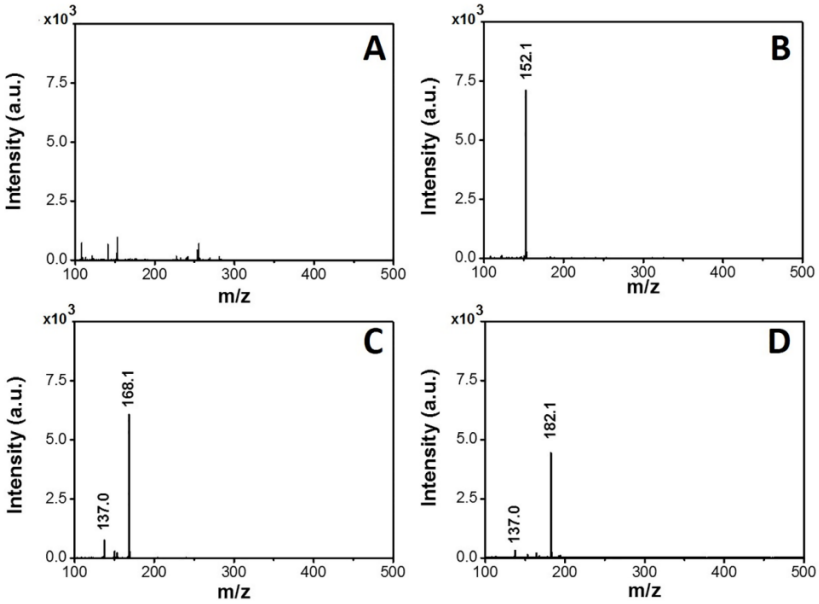

Fig S9. SALDI-MS spectras of A) blank, B) Da ([M-H]$^-$, m/z 152.1), C) Ne ([M-H]$^-$, m/z 168.1; [M-H_2O-H]$^-$, m/z 150.1; [M-CH_2NH_2-H]$^-$, m/z 137.0), D) E ([M-H]$^-$, m/z 182.1; [M-$CH_3CH_2NH_2$-H]$^-$, m/z 137.0). Matrix: ZrO_2-NPC-700. Detection: *Negative ion mode*. Laser conditions: 30 %, 500 shots. N=10

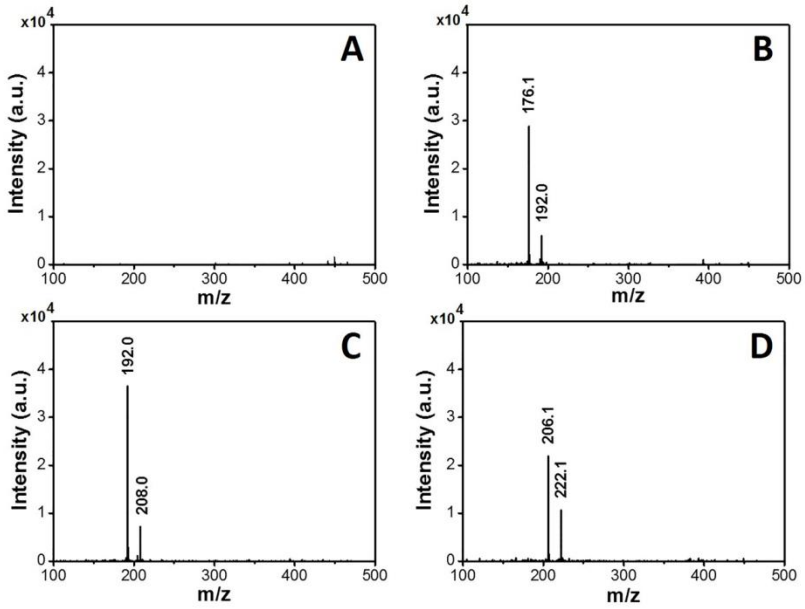

Fig S10. SALDI-MS spectras of A) blank, B) Da ([M+Na]$^+$, m/z 176.1; [M+K]$^+$, m/z 192.0), C) Ne ([M+Na]$^+$, m/z 192.0; [M+K]$^+$, m/z 208.0), D) E ([M+Na]$^+$, m/z 206.1; [M+K]$^+$, m/z 222.1). Matrix: ZrO_2-NPC-800ºC. Detection: *Positive ion mode*. Laser conditions: 30 %, 500 shots. N=10

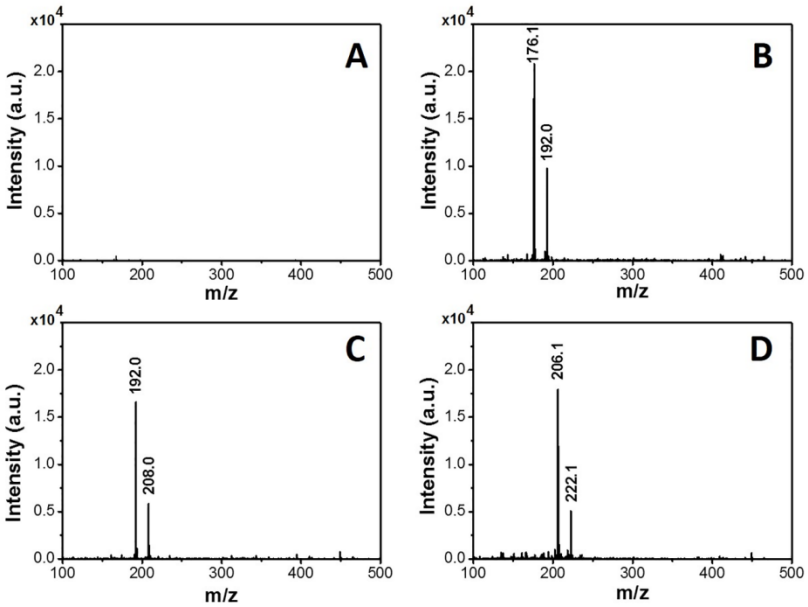

Fig S11. SALDI-MS spectras of A) blank, B) Da ($[M+Na]^+$, m/z 176.1; $[M+K]^+$, m/z 192.0), D) Ne ($[M+Na]^+$, m/z 192.0; $[M+K]^+$, m/z 208.0), E) E ($[M+Na]^+$, m/z 206.1; $[M+K]^+$, m/z 222.1). Matrix: ZrO_2-NPC-900ºC. Detection: *Positive ion mode*. Laser conditions: 30 %, 500 shots. N=10

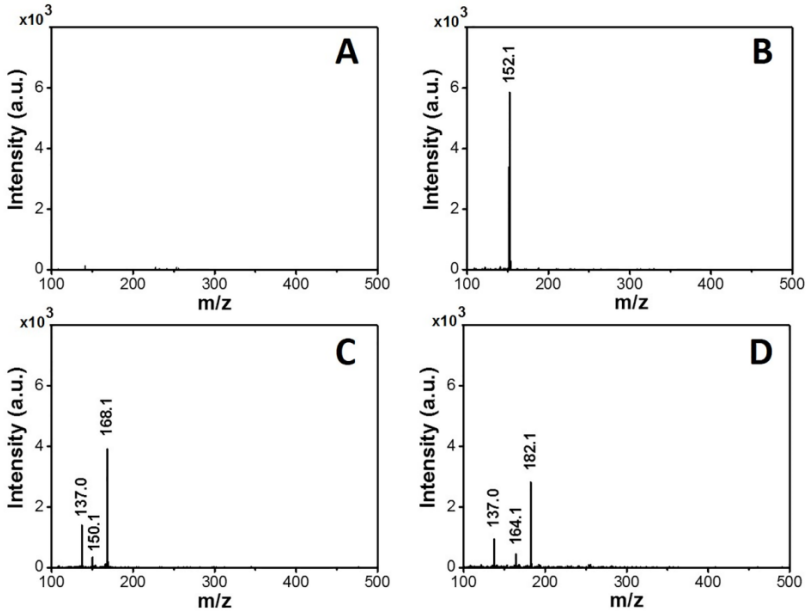

Fig S12. SALDI-MS spectras of A) blank, B) Da ($[M-H]^-$, m/z 152.1), C) Ne ($[M-H]^-$, m/z 168.1; $[M-H_2O-H]^-$, m/z 150.1; $[M-CH_2NH_2-H]^-$, m/z 137.0), D) E ($[M-H]^-$, m/z 182.1; $[M-H_2O-H]^-$, m/z 164.1; $[M-CH_3CH_2NH_2-H]^-$, m/z 137.0). Matrix: ZrO_2-NPC-900ºC. Detection: *Negative ion mode*. Laser conditions: 30 %, 500 shots. N=10

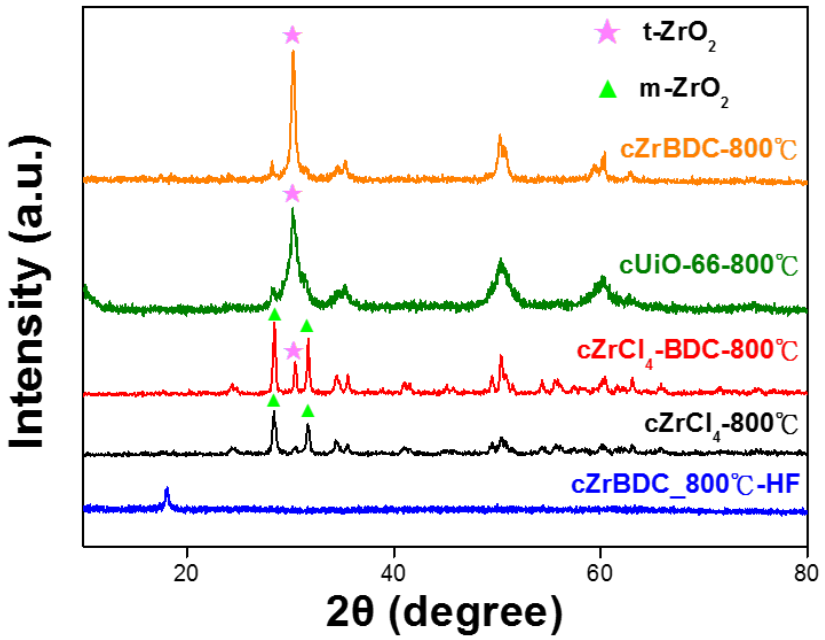

Fig. S13 PXRD patterns of the precursor of MOGs and cZrBDC-800 ºC with 10%HF.

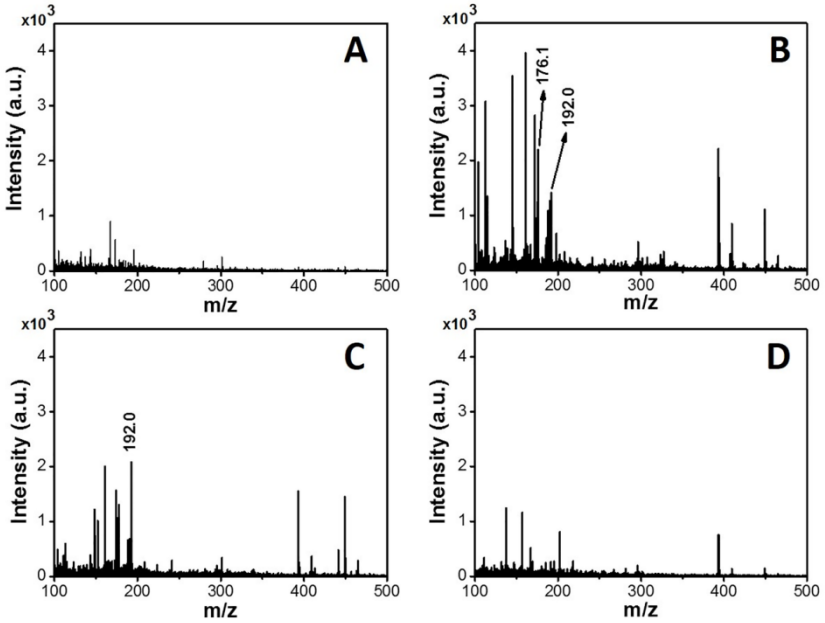

Fig. S14. SALDI-MS spectras of A) blank, B) Da ($[M+Na]^+$, m/z 176.1; $[M+K]^+$, m/z 192.0), D) Ne ($[M+Na]^+$, m/z 192.0), E) E (not detected). Matrix: ZrO_2-NPC-800 pretreated with 10 % HF. Detection: *Positive ion mode*. Laser conditions: 30 %, 500 shots. N=10

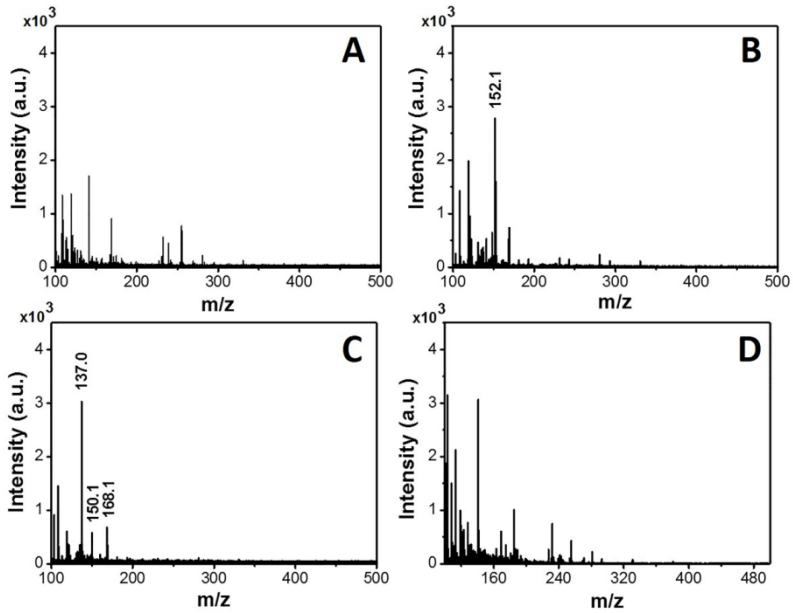

Fig. S15. SALDI-MS spectras of A) blank, B) Da ([M-H]$^-$, m/z 152.1), C) Ne ([M-H]$^-$, m/z 168.1; [M-H_2O-H]$^-$, m/z 150.1; [M-CH_2NH_2-H]$^-$, m/z 137.0), D) E (not detected). Matrix: ZrO_2-NPC-800 pretreated with 10 % HF. Detection: *Negative mode*. Laser conditions: 30 %, 500 shots. N=10

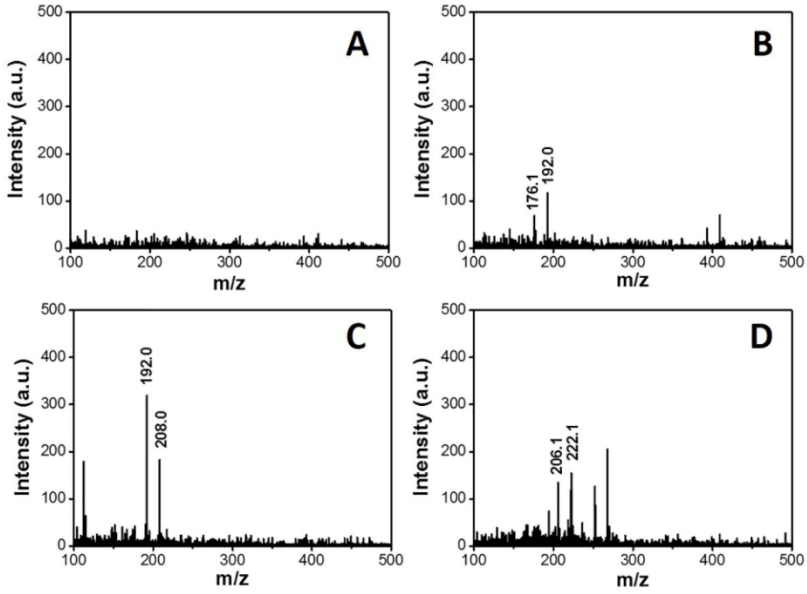

Fig S16. SALDI-MS spectras of A) blank, B) Da ([M+Na]$^+$, m/z 176.1; [M+K]$^+$, m/z 192.0), C) Ne ([M+Na]$^+$, m/z 192.0; [M+K]$^+$, m/z 208.0), D) E ([M+Na]$^+$, m/z 206.1; [M+K]$^+$, m/z 222.1). Matrix: $cZrCl_4$-BDC-800. Detection: *Positive ion mode*. Laser conditions: 30 %, 500 shots. N=10

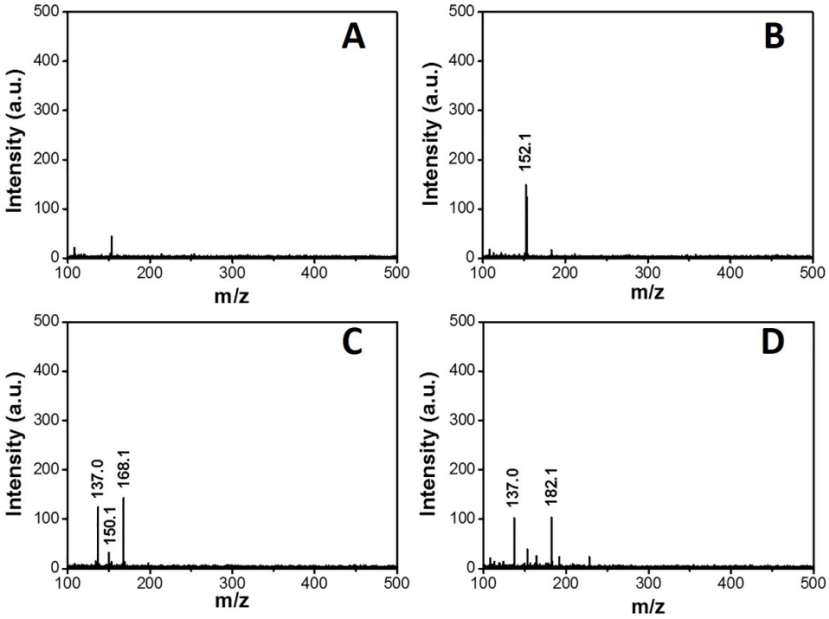

Fig S17. SALDI-MS spectras of A) blank, B) Da ([M-H]$^-$, m/z 152.1), C) Ne ([M-H]$^-$, m/z 168.1; [M-H_2O-H]$^-$, m/z 150.1; [M-CH_2NH_2-H]$^-$, m/z 137.0), D) E ([M-H]$^-$, m/z 182.1; [M-$CH_3CH_2NH_2$-H]$^-$, m/z 137.0). Matrix: c$ZrCl_4$-BDC-800. Detection: *Negative ion mode*. Laser conditions: 30 %, 500 shots. N=10

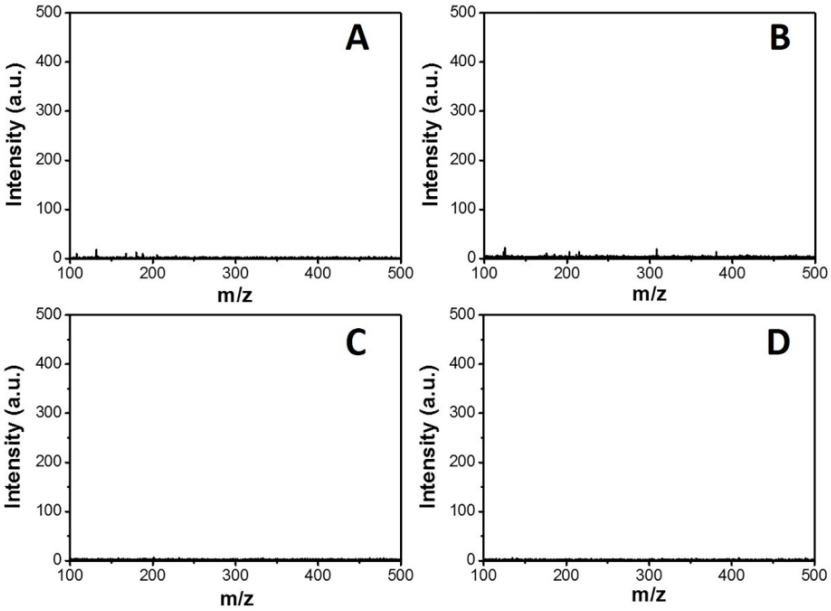

Fig S18. SALDI-MS spectras of A) blank and B) 100 ppm catecholamines detected at *positive ion mode*; C) blank and D) 100 ppm catecholamines detected at *negative ion mode*. Matrix: c$ZrCl_4$-800. Laser conditions: 30 %, 500 shots. Catecholamines contained: Da, Ne and E. N=10

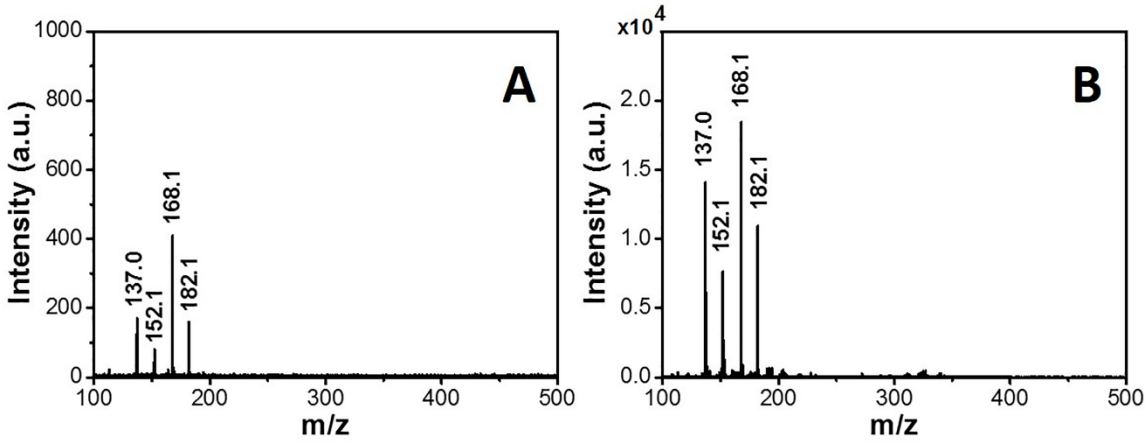

Fig S19. Comparison of SALDI-MS spectras of A) cUiO-66-800 and B) ZrO_2-NPC-800 as matrix. Da ([M-H]-, m/z 152.1), Ne ([M-H]-, m/z 168.1; [M-H_2O-H]-, m/z 150.1; [M-CH_2NH_2-H]-, m/z 137.0), E ([M-H]-, m/z 182.1; [M-$CH_3CH_2NH_2$-H]-, m/z 137.0). Detection: *Negative ion mode*. Laser conditions: 30 %, 500 shots. N=10

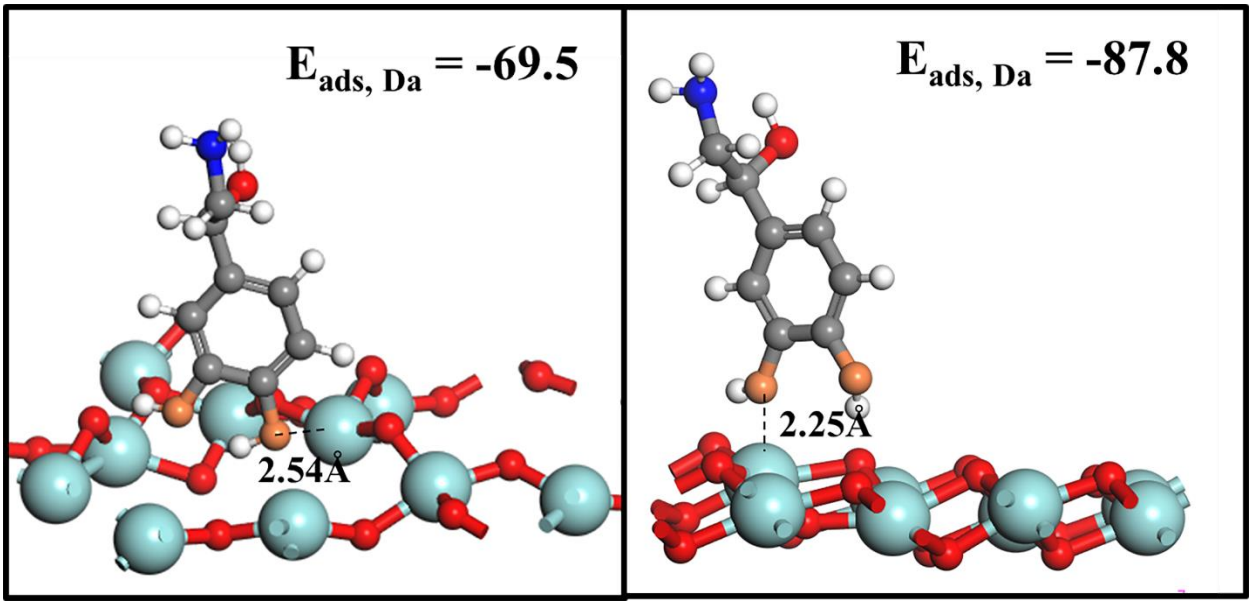

Fig S20. DFT calculated adsorption sites for Da in *m*-ZrO_2 (left) and *t*-ZrO_2 (right). Adsorption energies (E_{ads}) are in kJ mol^{-1}. The atoms are shown as follows: Zr-green, H-white, O-red, C-gray, N-blue, O in catechol-orange.

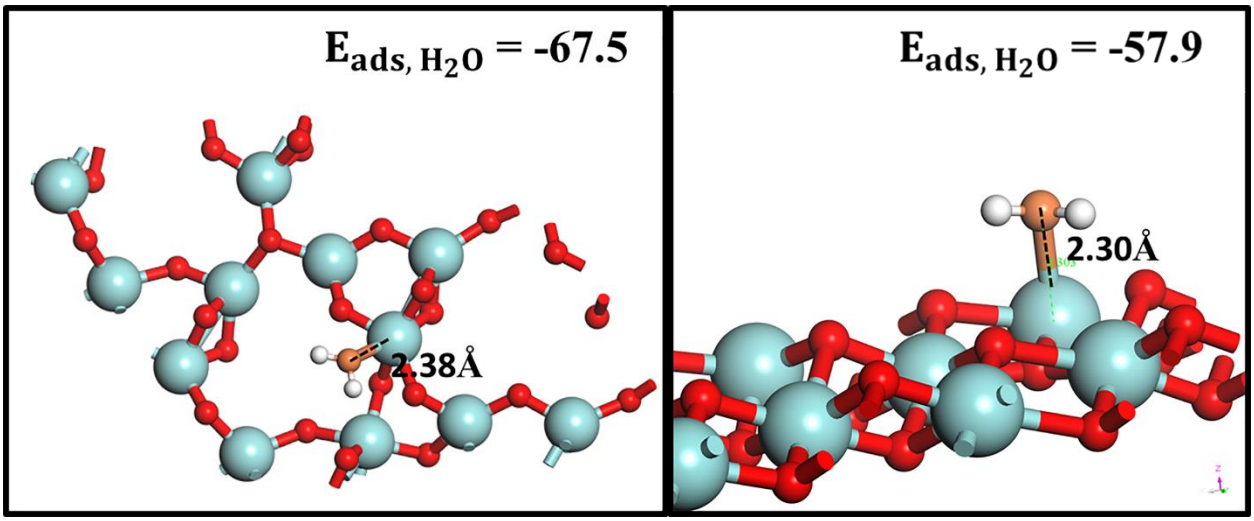

Fig S21. DFT calculated adsorption sites for H_2O in m-ZrO_2 (left) and t-ZrO_2 (right). Adsorption energies (E_{ads}) are in kJ mol^{-1}. The atoms are shown as follows: Zr-green, H-white, O-red, C-gray, O in water-orange.

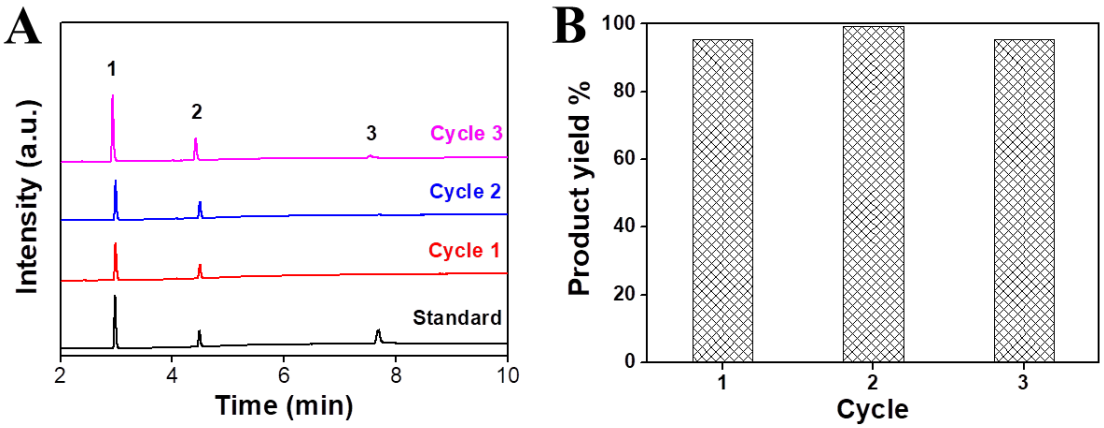

Fig. S22 A) GC-FID chromatogram of obtained from the transesterifcation reaction of palmitic acid and methanol. B) Reutilization of ZrO_2-NPC-800 of three transesterification reactions. Condition: The product was obtained after 24 h of reaction at 68 °C, using 18 wt.% of ZrO_2-NPC-800ºC as catalyst. 1= methyl palmitate, 2=methyl linoleate (internal standard) and 3=palmitate.

Table S1. SEM-EDS analysis of the MOG, carbonized MOG at different temperatures and cUiO-66

Materials	Weight percent (%)			
	C	O	Si	Zr
Zr-MOG	53.7	16.8	12.7	16.8
ZrO_2-NPC-600	20.9	24.2	9.6	45.3
ZrO_2-NPC-700	29.4	25.7	6.7	38.2
ZrO_2-NPC-800	40.0	17.6	11.5	30.9
cUiO-66-800	*31.6*	*18.9*	*11.3*	*38.2*
ZrO_2-NPC-900	32.8	21.7	7.3	38.2

Table S2. Surface area and pore size distribution of Zr-MOG and ZrO_2-NPCs at specified temperature

Materials	Surface area (m^2/g)[a]	Pore size (nm)
Zr-MOG	690.3	1.37
ZrO_2-NPC-600[b]	193.6	0.6
ZrO_2-NPC-700[c]	330.8	1.1, 1.8-2.6
ZrO_2-NPC-800[d]	495.9	1.1, 2.1-3.7
ZrO_2-NPC-900[e]	341.7	0.8-1.4, 2.3-4.0

[a]Experimental data were calculated *via* BET method.

The carbonization temperatures were carried out at [b]600 ºC, [c]700 ºC, [d]800 ºC, and [e]900 ºC.

Table S3. LDI performance of ZrO_2-NPCs for neurotransmitters[a]

Matrices	S/N ratio (% RSD)[b]		
	Ne	**Da**	**E**
ZrO_2-NPC-600	284 (16)	1223 (9)	921 (9)
ZrO_2-NPC-700	236 (12)	923 (10)	923 (10)
ZrO_2-NPC-800	350 (9)	1912 (7)	1112 (8)
ZrO_2-NPC-900	673 (5)	1976 (3)	1977 (2)

[a]Detected at positive ion mode, [b]RSD = relative standard deviation (N=10)

Table S4. LDI performance of ZrO_2-NPCs for neurotransmitters[a]

Matrices	S/N ratio (% RSD)[b]		
	Ne	**Da**	**E**
ZrO_2-NPC-600	1249 (8)	1383 (6)	819 (5)
ZrO_2-NPC-700	1560 (6)	1688 (11)	905 (9)
ZrO_2-NPC-800	3613 (5)	3679 (5)	2363 (9)
ZrO_2-NPC-900	1190 (5)	1614 (4)	745 (3)
cUiO-66-800	*296 (17)*	*163 (15)*	*182 (20)*

[a]Detected at negative ion mode, [b]RSD = relative standard deviation (N=10)

Table S5. LDI performance of MOG precursors and ZrO_2-NPC-800

Analytes	S/N ratio (RSD)[a]			
	ZrO_2-NPC-800	$cZrCl_4$-800	$cZrCl_4$-BDC-800	cUiO-66-800
Ne	3613 (5)	n.d[b]	44 (11.3)	296 (17)
Da	3679 (5)	n.d[b]	46 (14.8)	163 (15)
E	2363 (9)	n.d[b]	32 (19.2)	182 (20)

[a] Relative standard deviation, [b]not detected, N=10. Laser conditions: 30 %, 500 shots. N=10

Table S6. Analytical performance of other reported matrices applied for the LDI of neurotransmitters.

Matrices	**Analytes**	**Detection limit**	**RSD[a]**	**Refs**
$[TiO_2\text{-}Si\text{-}NH_3^+][CHC^-]$	dopamine	-[a]	-[a]	S2
porous silicon dioxide	dopamine	0.65 uM	-[a]	S3
Hydroxyethyl Methacrylate-Functionalized Graphene Oxide	dopamine	0.13 uM	-[a]	S4
3-CF_3-BTD[b]	dopamine epinephrine	3.27 uM 10 uM	-[a]	S5
DHPT[c]	dopamine	> 10 uM	> 2 %	S6
Carbon dots	dopamine	5 nM	9.4 %	S7
ZrO_2-NPC-800[d]	dopamine	0.53 nM	5.0 %	This work

[a]Not reported, [b]5-(3-trifluoromethylbenzylidene)thiazolidine-2,4-dione, [c]2,3,4,5-Tetrakis(3',4'-dihydroxylphenyl)thiophene, [d]N=10.

Table S7. Analytical performance of the optimized ZrO_2-NPC-800 for LDI process of neurotransmitters.

Analytes	Limit of detection (LOD)[a]	
	Positive ion mode	Negative ion mode
Ne	5.1 nM	0.49 nM
Da	1.0 nM	0.53 nM
E	1.5 nM	0.69 nM

[a]Laser conditions: 30 %, 500 shots. N=10

Table S8. Transesterification of palmitic acid using ZrO_2-NPC-800 as catalyst

Reaction times	**Conversion (%)**
Cycle 1	95
Cycle 2	99
Cycle 3	95

Reaction conditions: The product was obtained after 24 h of reaction at 68 °C, using 18 wt.% of ZrO_2-NPC-800 as catalyst.

References:

(1) L. Liu, J. Zhang, H. Fang, L. Chen and C. Y. Su, *Chemistry – An Asian Journal*., 2016, **11**, 2278-2283.

(2) H. Liu, J. Dai, J. Zhou, H. Huang, F. Chen and Z. Liu., *Int. J. Mass Spectrom.,* **2015,** *376*, 85-89.

(3) A. Kraj, J. Jarzebinska, A. Gorecka Drzazga, J. Dziuban and J. Silberring. *Rapid Commun. Mass Spectrom.*, **2006**, *20*, 1969-1972.

(4) X. Zheng, J. Zhang, H. Wei, H. Chen, Y. Tian and J. Zhang. *Anal. Lett.*, **2016**, *49*,1847-1861.

(5) H. Kasai, M. Nakakoshi, T. Sugita, M. Matsuoka, Y. Yamazaki, Y. Unno, H. Nakajima, H. Fujiwake and M. Tsubuki, *Anal. Sci.*, **2016**, *32*, 907-910.

(6) S. Chen, L. Chen, J. Wang, J. Hou, Q. He, J. A. Liu, J. Wang, S. Xiong, G. Yang and Z. Nie, *Anal. Chem.*, **2012**, *84*,10291-10297.

(7) M. S. Khan, M. L. Bhaisare, S. Pandey, A. Talib, S. M. Wu, S. K. Kailasa and H. F. Wu, *Int. J. Mass Spectrom.*, **2015,** *393*, 25-33.